JOURNAL OF MATERIALS SCIENCE 12 (1977) 341–346

Carrier recombination at dislocations in epitaxial gallium phosphide layers

J. M. TITCHMARSH, G. R. BOOKER
Department of Metallurgy and Science of Materials, University of Oxford, Oxford, UK
W. HARDING, D. R. WIGHT
Services Electronics Research Laboratories, Baldock, Herts, UK

The nature of dark spots observed in cathodoluminescence micrographs of gallium phosphide epitaxial layers has been examined using the transmission electron microscope and etching studies. Each dark spot is shown to be located at the intersection of a dislocation with the layer surface. Moreover screw, edge and mixed dislocations all give rise to spots of similar size and intensity. It is suggested that enhanced non-radiative recombination which gives rise to the dark spots is due to the core structure, rather than a concentration of dopant atoms, method of layer growth, etc., and that different core structures are equally effective.

1. Introduction

There is interest at present in increasing the efficiency of GaP green light-emitting diodes (LEDs). Such diodes are generally made using either vapour-phase epitaxy (VPE) or liquid-phase epitaxy (LPE) GaP layers grown on pulled single-crystal GaP substrates, the layers containing suitable dopants and nitrogen. The nitrogen provides efficient isoelectronic radiative recombination centres, which have to compete with the non-radiative recombination centres present in the material. Recent work has shown that poor diode efficiencies are often associated with high densities of grown-in dislocations [1, 2].

For good diode efficiencies, the epitaxial layers should possess good luminescence properties before the diodes are fabricated, as indicated by either high bulk photoluminescence (PL) efficiency [3] or high bulk cathodoluminescence (CL) efficiency [4]. Both of these luminescence efficiencies, η, are proportional to the minority carrier lifetime, τ, for the particular material [3, 5]. The lifetime, τ, in turn depends on the density, ρ, of grown-in dislocations when ρ is sufficiently large [6–8]. This occurs because as ρ increases, the mean distance d between dislocations decreases, and when d becomes comparable with the minority carrier diffusion length L for the corresponding low dislocation density material, the dislocations then control both L and τ, i.e. the dislocations become the dominant non-radiative recombination centre. Consequently, as ρ increases, τ decreases, and this causes η to decrease, and hence also the diode efficiency. In one investigation τ was also shown to be proportional to the concentration of a trap located 0.75 eV above the valence band [5], and it is tempting to associate this trap with the grown-in dislocations. Work on materials other than GaP has also shown that τ decreases as ρ increases e.g. on Ge [9, 10], Si [10, 11] and GaAs [12].

Direct evidence for non-radiative recombination occurring at individual dislocations in GaP has been obtained by recording micrographs using either electroluminescence (EL) [1], CL [2, 13] or PL [16] signals to give the images. In such micrographs, the individual dislocations appear as dark spots. Similar micrographs were also obtained from GaP by using the electron beam induced conductivity signal [1]. For all of these microscopic techniques, the dark spots were correlated with grown-in dislocations either from the general appearance of the dark spot distributions, or more rigorously by comparing the dark spots with etch pits in micrographs obtained from the same speci-

men areas. Work on materials other than GaP has revealed dark spots in micrographs using similar techniques, e.g. on Si [14], GaAs [15–18] and GaAsP [19].

Although the factors controlling the efficiencies of green LEDs are now better understood, some points still need resolving if complete quantitative assessments are to be made. It is especially important to establish whether all types of dislocations, e.g. screw, 30°, 60°, edge, etc., are equally effective in acting as non-radiative recombination centres [2]. This is still uncertain because although there is a definite correlation between dark spots and etch pits, there is still doubt as to whether etching reveals all of the dislocations present [2]. Furthermore, etching does not enable one to distinguish between the different types of dislocation.

In order to obtain further information on this point, a combined CL, transmission electron microscope (TEM) and etch pit study has been made of several GaP epitaxial layer specimens. The main result of the investigation was that many different types of dislocation were present, and that all were extremely effective in acting as non-radiative recombination centres.

2. Cathodoluminescence studies

A range of epitaxial material was selected for investigation, including LPE layers grown in a horizontal furnace onto (1 1 1) or (1 0 0) orientated pulled-crystal substrates; sample dimensions were typically 2 to 4 mm. *P*-type layers were doped with Zn ($N_A - N_D \sim 5 \times 10^{17}$ cm^{-3}), and *n*-type layers were undoped or doped with S, Te or Si (1×10^{14} cm$^{-3} < N_D - N_A < 1 \times 10^{18}$ cm^{-3}). Some samples had been nitrogen-doped (concentration $< 10^{18}$ cm^{-3}) by adding gaseous NH_3 to the hydrogen atmosphere in the furnace. A number of sulphur-doped, *n*-type, VPE layers* with and without nitrogen doping were also studied.

CL micrographs were obtained using a scanning electron microscope (Cambridge Stereoscan Mark IIA) with a specially developed CL mode detection system. A beam voltage of 30 kV was employed with probe currents in the range 10^{-7} to 10^{-6} A and probe size 0.5 μm diameter. The beam was incident normally on the sample's surface and the luminescence output was collected by a mirror system and detected with a photomultiplier tube (EMI 9658B S20 cathode), green luminescence being selected with an interference filter.

A typical CL micrograph exhibiting dark spots is shown in Fig. 1. All the materials studied showed these features, although in a few instances some dark lines and/or more random shapes were present. In samples showing clearly defined, approximately circular spots, the densities of the features were in general variable across the surface of the epitaxial layer, although many samples showed a more or less uniform distribution. The dark spots were typically 5 to 7 μm diameter, and the density ranged from 5×10^3 to 10^6 cm^{-2}.

Two samples with high luminescence efficiencies were selected for detailed study. (a) A (1 0 0) oriented, Si-doped, *n*-type ($n = 1.0 \times 10^{18}$ cm^{-3}), LPE sample with a layer thickness of 70 μm, and (b) a (1 1 1)A oriented, Te-doped ($N_D - N_A = 1.3 \times 10^{18}$ cm^{-3}) LPE sample with a layer of thickness 95 μm. The first sample was used to correlate the dark spots present in CL micrographs with dislocations observed using the TEM. The second sample was used to correlate the dark spots with etch pits.

3. Transmission electron microscope studies

To obtain an exact correlation of the dark spots with dislocations, it was necessary first to record CL micrographs of a specific area of the sample, and then to prepare a TEM specimen by thinning the sample in that same area, from the substrate side only, to a thickness of about 1 μm. Secondary electron emissive mode micrographs were recorded,

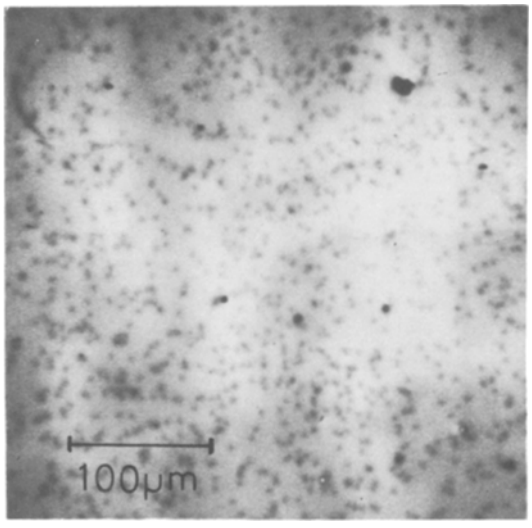

Figure 1 A typical CL micrograph of a GaP epitaxial layer with a dark spot density of approximately 5×10^5 cm^{-2}.

*Kindly supplied by Dr P. Hart, Allen Clark Research Laboratories, Plessey Co, Ltd, Towcester, UK.

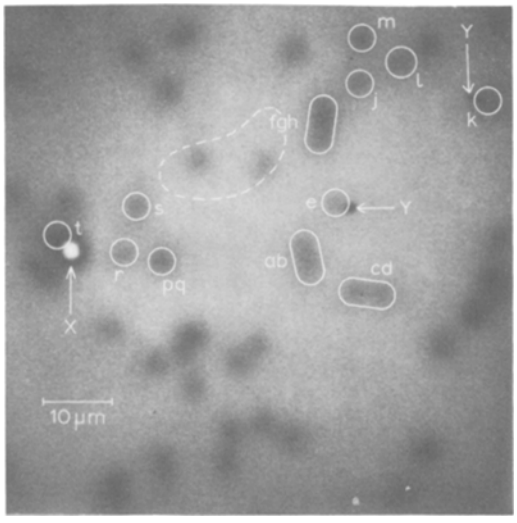

Figure 2 A CL micrograph of a (1 0 0) oriented Si-doped GaP layer. The dashed line marks the position of a hole produced during the TEM specimen preparation of this same area. The feature marked X is a pinhole in the epitaxial layer and those marked Y are small particles of dirt. The remaining letters refer to dark spots.

corresponding to each CL micrograph, and the surface features in these micrographs registered with surface features observed in optical micrographs. The sample was then thinned by chemical jet polishing, using a solution of chlorine gas dissolved in methanol, until small holes appeared. More emissive mode and optical micrographs were recorded, and these enabled the positions of the holes to be drawn accurately on the CL micrographs.

Fig. 2 shows a CL micrograph with the position of a subsequently formed hole indicated by the dashed line. The bright feature X corresponds to a pinhole in the epitaxial layer, and the dark feature Y to a small particle of dirt subsequently removed during the TEM specimen preparation. The area surrounding the hole and containing a number of dark spots was examined in an AEI EM7 electron microscope operating at 500 kV.

The only structural features observed using the TEM were dislocations which threaded the foil. A low-magnification montage of transmission electron micrographs (Fig. 3) was constructed so that the positions of a number of dislocations could be registered with respect to the position of the hole in the specimen and the pinhole X (Fig. 2). Additional dislocations which had been out of contrast under the diffraction conditions used to record

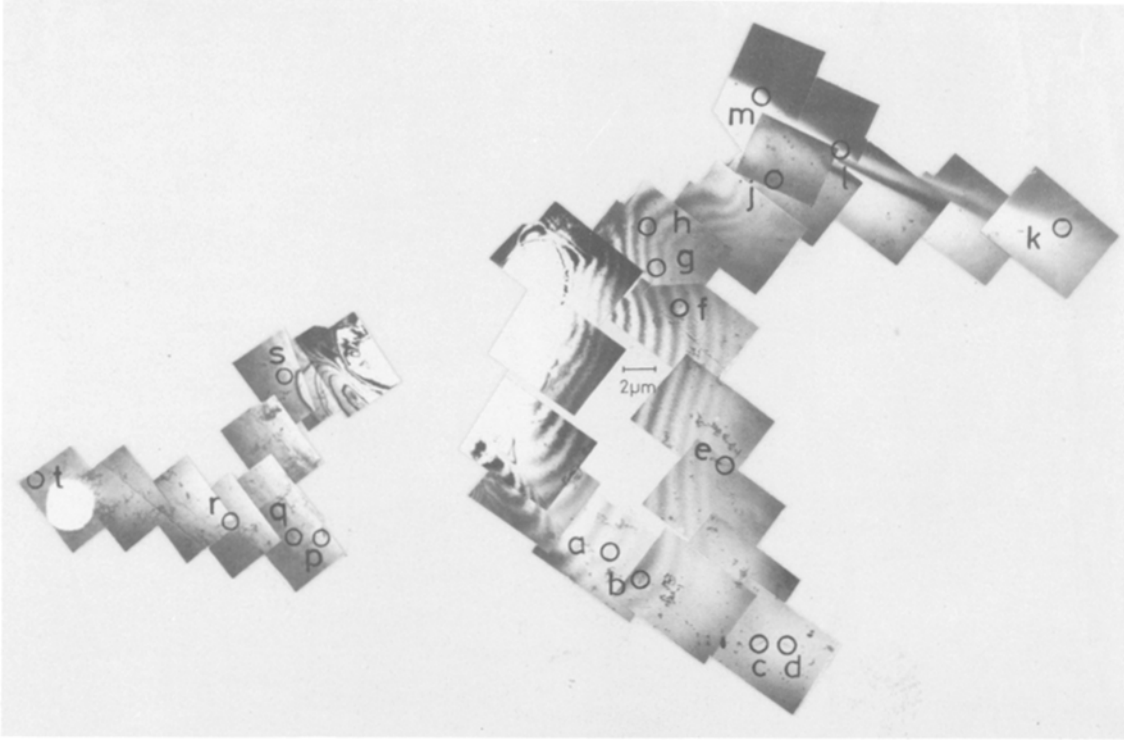

Figure 3 A low-magnification TEM micrograph montage of part of the same area shown in Fig. 2. The lettered circles mark the positions of dislocations in the thin foil and these can be compared with the positions of the lettered dark spots in Fig. 2.

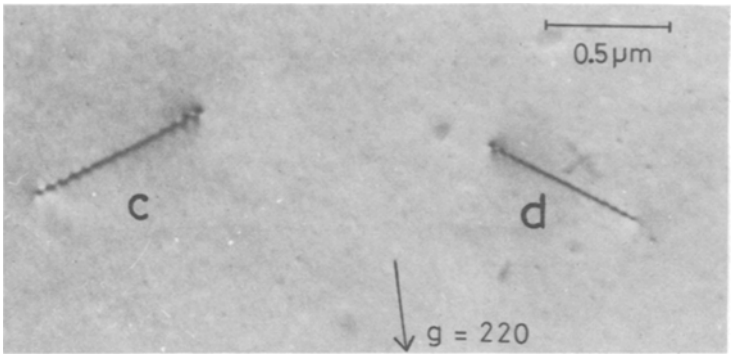

Figure 4 A higher magnification TEM micrograph of two dislocations which show typical oscillating contrast but no obvious precipitation.

Fig. 3, were observed when the foil was re-examined using different diffracting conditions. Some of the dislocations were seen better when the foil was tilted through large angles ($>30°$), these dislocations had been previously viewed end-on in Fig. 3 and were less readily visible. Fig. 4 shows two of the dislocations at higher magnification. There was no evidence of precipitation on the dislocations, although an impurity atmosphere surrounding the dislocations could have been present without being detected by the TEM examination.

In every case it was found that a dislocation corresponded to a dark spot, and vice-versa. A number of dark spots in Fig. 2 have been circled and lettered for comparison with Fig. 3. Each of the extended dark spots ab and cd in Fig. 2 correspond to two dislocations about 3 μm apart, whilst fgh in Fig. 3 corresponds to three dislocations with similar separations. The spot lettered pg (Fig. 2) is much darker than the others, and two dislocations less than 2 μm apart were observed at that point.

Slight displacements of 1 or 2 μm were sometimes observed between the two corresponding positions in the CL and TEM micrographs, and this can be at least partly explained in the following manner. Contrast in the CL mode depends upon the depth of penetration of the incident electron beam, which is several microns for the beam potential of 30 kV used in these experiments. Thus, the centre of the dark spots probably corresponds to the position of the dislocation typically 1 to 2 μm below the epitaxial layer surface. For a dislocation inclined at 45° to the plane of the foil, this would give a displacement of 1 to 2 μm relative to the point of termination of the dislocation in the specimen surface.

The nature of the seventeen dislocations lettered in Fig. 3 were analysed in detail and the results are given in Table I. All were perfect dislocations with $a/2\langle 1\,1\,0\rangle$ Burgers vectors. Among the seventeen, five of the possible six different types of $a/2\langle 1\,1\,0\rangle$ Burgers vectors were present ($+\boldsymbol{b}$ and $-\boldsymbol{b}$ were not distinguished). The crystallographic directions of the dislocation lines were deduced from stereomicrographs and careful tilting experiments, and it was found that screw, edge and mixed dislocations were all present. Dislocations were observed at positions corresponding to the unlettered dark spots in Fig. 2, but Burgers vectors were not determined for these dislocations.

4. Etch pit studies

A CL micrograph (Fig. 5a) of the (1 1 1)A oriented sample selected for this study showed a typical

TABLE I Burgers vector analyses of dislocations

Dislocation letter in Fig. 3	Burgers vector*	Dislocation* axis	Dislocation type
a	$a/2[1\bar{1}0]$	[0 0 1]	90°
b	$a/2[0\,1\,\bar{1}]$	†$[1\,1\,\bar{2}]\rightarrow[0\,\bar{1}\,1]$	0→30°
c	$a/2[0\,1\,\bar{1}]$	†$[1\,\bar{1}\,2]\rightarrow[0\,\bar{1}\,1]$	0→30°
d	$a/2[1\,0\,\bar{1}]$	†$[\bar{1}\,1\,2]\rightarrow[1\,0\,\bar{1}]$	0→30°
e	$a/2[0\,1\,\bar{1}]$	$[1\,\bar{1}\,2]$	30°
f	$a/2[0\,1\,\bar{1}]$	$[0\,1\,\bar{1}]$	0°
g	$a/2[1\,1\,0]$	[0 0 1]	90°
h	$a/2[1\,0\,\bar{1}]$	†$[1\,0\,\bar{1}]\rightarrow[\bar{1}\,1\,2]$	0→30°
j	$a/2[0\,1\,\bar{1}]$	$[0\,1\,\bar{1}]$	0°
k	$a/2[0\,1\,\bar{1}]$	$[0\,1\,\bar{1}]$	0°
l	$a/2[1\,1\,0]$	[0 0 1]	90°
m	$a/2[1\,1\,0]$	[0 0 1]	90°
p	$a/2[1\,0\,1]$	[0 0 1]	45°
q	$a/2[1\,0\,\bar{1}]$	†$[\bar{1}\,1\,2]\rightarrow[1\,0\,\bar{1}]$	0→30°
r	$a/2[1\,1\,0]$	$[0\,\bar{1}\,1]$	60°
s	$a/2[0\,1\,\bar{1}]$	†$[0\,1\,1]\rightarrow[1\,\bar{1}\,2]$	0→30°
t	$a/2[1\,0\,1]$	[1 0 1]	0°

* A right-handed axis system is used with the foil normal [0 0 1]

† These dislocations do not lie exactly along low-index crystallographic directions, but between the two directions indicated and on the [1 1 1] slip planes containing these directions.

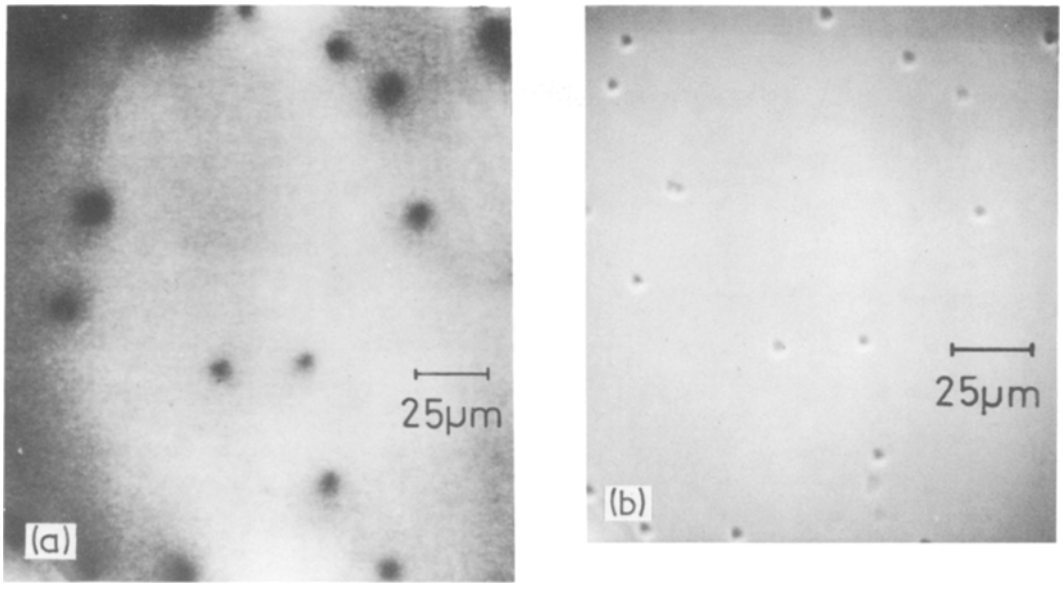

Figure 5 (a) A CL micrograph of the (1 1 1)A oriented Te-doped layer, and (b) the same area after etching to reveal dislocation sites imaged in the secondary electron mode of the SEM.

array of dark spots. The secondary electron emissive mode micrograph indicated that the specimen surface in this area was featureless.

The specimen was etched for 16 sec in an aqueous solution of KOH ($120\,g\,l^{-1}$) and $K_3Fe(CN)_6$ ($80\,g\,l^{-1}$) heated to its boiling point, and the area shown in Fig. 5a re-examined. The emissive mode micrograph (Fig. 5b) showed clearly defined triangular etch pits which correlated with the positions of the dark spots in Fig. 5a. A few less well defined, shallower etch features were present which do not correlate with dark spots. The triangular pits are typical of dislocations, and the one-to-one correspondence between dark spots and dislocations obtained in Section 3 is thus confirmed by these etching studies. The two sets are in register to within $2\,\mu m$, and the slight displacements ($< 2\,\mu m$) can probably be explained either by the removal of material during etching or by the effect due to the penetration of the electron beam described above.

5. Discussion

The combined CL and TEM examination of the same area of the GaP specimen has demonstrated conclusively there is a one-to-one correspondence between the CL dark spots and the dislocations emerging at the specimen surface. Each dark spot contained a dislocation, and each dislocation gave a dark spot. The only exception was when the dislocations were too close together ($< 5\,\mu m$) for the dark spots to be resolved. The dark spots then either ran together to give elongated spots or became superimposed to give darker spots. A dark spot occurred regardless of the type of dislocation, i.e. whether screw, 30°, 60° or edge.

Two possible mechanisms may explain the effect of dislocations as non-radiative recombination centres. The recombination may be due either to some interaction between the dislocations and impurities or point defects, or to a property of the dislocations themselves. The experimental results show that grown-in dislocations act as recombination centres in epitaxial material regardless of the method and temperature of growth, the type and concentration of dopant, or the crystallographic orientation. This suggests that neither impurity nor native defect (e.g. interstitial Ga or P atoms, or vacancies) interactions are the main reason for recombination behaviour. The results of Heinke and Queisser [18] in GaAs do not contradict this view, their investigation showing that interactions with impurities or point defects decrease the effectiveness of dislocations as non-radiative recombination centres.

If the effect is due mainly to the core or elastic strain field of the dislocations, then it might be expected to depend on the type of dislocation. The experimental results provide no evidence for this. A possible explanation may be that the diff-

erent types of dislocations have different capture radii, different lifetimes in the captured state etc., but nevertheless all the types compete effectively with the recombination processes in the bulk of the crystal and hence appear similar in the present studies.

The present work does not enable the dominant mechanism to be determined, but the overall results tend to suggest that it is an inherent property of the dislocation rather than a mechanism involving the interaction of impurities or point defects with the dislocation.

Acknowledgements

We acknowledge the assistance of I. D. Blenkinsop and D. Dosser. The work has been carried out with the support of the Procurement Executive, Ministry of Defence.

References

1. G.B. STRINGFELLOW, P.F. LINDQUIST, T.R. CASS and R. A. BURMEISTER, *J. Electron. Mater.* **3** (1974) 497.
2. W.A. BRANTLEY, O.G. LORIMER, P.D. DAPKUS, S. E. HASZKO and R. H. SAUL, *J. Appl. Phys.* **46** (1975) 2629.
3. P. D. DAPKUS, W. H. HACKETT, O. G. LORIMER, G. W. KAMMLOTT and S. E. HASZKO, *Appl. Phys. Letters* **22** (1973) 227.
4. D.R. WIGHT, J.C.H. BIRBECK, J.W.A. TRUSSLER and M. L. YOUNG, *J. Phys. D.* **6** (1973) 1622.
5. B. HAMILTON, A. R. PEAKER, S. BRAMWELL, W. HARDING and D. R. WIGHT, *Appl. Phys. Letters* **26** (1975) 702.
6. T. SUZUKI and Y. MATSUMOTO, *ibid* **26** (1975) 431.
7. I. D. BLENKINSOP, W. HARDING and D. R. WIGHT, reported by P. J. Dean at International Conference on Luminescence, Japan, September 1975, *J. Luminescence* **12/13** (1976) 83.
8. F. P. G. KUIJPERS, L. BLOK and A. T. VINK, International Conference on Luminescence, Japan, September 1975, in press.
9. J. OKADA, *J. Phys. Soc. Japan* **10** (1955) 1110.
10. A. D. KURTZ, S. A. KULIN and B. L. AVERBACH, *Phys. Rev.* **101** (1956) 1285.
11. D. R. HUNTER, D. H. PAXMAN, M. BURGESS and G. R. BOOKER, "Scanning Electron Microscopy: Systems and Applications 1973", edited by W. C. Nixon, Conference Series No. 18, (Institute of Physics, London and Bristol), p. 208.
12. M. ETTENBERG, *J. Appl. Phys.* **45** (1974) 901.
13. S.M. DAVIDSON, M.A. IQBAL and D.C. NORTHROP, *Phys. Stat. Sol. A* **29** (1975) 571.
14. W. CZAJA and J. R. PATEL, *J. Appl. Phys.* **36** (1965) 1476.
15. H. C. CASEY, *J. Electrochem. Soc.: Sol. Stat. Sci.* **114** (1967) 153.
16. K. H. ZSCHAUER, *Sol. Stat. Commun.* **7** (1969) 335.
17. A. L. ESQUIVEL, W. N. LIN and D. B. WITTRY, *Appl. Phys. Letters* **22** (1973) 414.
18. W. HEINKE and H. J. QUEISSER, *Phys. Rev. Letters* **33** (1974) 1082.
19. H. KASANO and S. HOSOKI, *J. Appl. Phys.* **46** (1975) 394.

Received 13 April and accepted 4 May 1976.